TWO- AND THREE-DIMENSIONAL TRANSIENT ANALYSIS OF FLOW AND HEAT TRANSFER IN STRUCTURES WITH DOMICAL AND CURVED ROOFS

Z. Altaç[1,*], N. Ugurlubilek[1]

ABSTRACT

The aim of this study is to investigate transient buoyancy driven free convection heat transfer in domical (with a dome) structures or curved roofs is numerically. Two- and three-dimensional turbulent free convection are considered for the Rayleigh number intervals ($10^8 \leq Ra \leq 10^{10}$). The aspect ratios of H/L=1 and 2, with respect to the heated length, are considered. The heating is provided from a lateral surface while cooling is from opposing lateral surface. The hot and cold surfaces are kept isothermal, and all other surfaces are adiabatic. The Boussineq approximation is used for modeling the buoyancy flow. The RNG k-ε turbulence model is used. The pertinent transient equations are solved using Fluent 6.3.26 software. The flow of air (streamlines) and temperature distribution (isotherms) are produced. The mean Nusselt number is evaluated over the isothermal hot wall is computed, and the results are analyzed with respect to the flow and geometric variations. The mean Nusselt number using the 2-D simulations indicate that the mean Nusselt number does not significantly change with H/L ratio. The 3-D simulations yield higher mean Nusselt numbers, but they are smaller than those of obtained for flat top enclosures.

Keywords: *Buoyancy Flow, Domical Structure, Natural Convection, Turbulent Heat Transfer*

INTRODUCTION

Semispherical or domical structures are encountered in the main infrastructures serving as observatory, nuclear power plant containment buildings, concert halls, sports centers, ice-rings, office buildings, factory halls, shopping centers, passenger terminal buildings, shrines, mosques or traditional middle eastern public buildings such as bazaars and market places.

These structures or buildings often present unsolved problems related to energy and air flow such as thermal stratification, local heating or uncontrolled contaminant spreading. Consequently, there exists no previous experience and very careful analysis of the ventilation design is advisable.

A large enclosure is defined as an enclosed ventilated air space partly occupied and containing various contaminant and heat sources. It is distinguished by the strong effect that buoyancy and temperature differences have on air-motion, in particular on vertical streams of warm or cold air. In large enclosures common ventilation strategies require considerable amounts of energy to move and condition enormous amounts of air. The air flow pattern should therefore be well-planned and controlled to ensure an acceptable indoor air quality in the occupied zone without the need for excessive air flow rates.

Some designs suffer both from over-sizing of equipment and from excessive energy requirements, which-are usually caused by the lack of theoretical knowledge and guidance at the design stage [1]. The techniques for the design and analysis of such structures are categorized mainly in two main groups according to the level of model details. The first group, macroscopic models, are simplified models for a first estimate add concept evaluation. The second group, microscopic models, are detailed, models for design evaluation and, troubleshooting, such as computational fluid dynamics (CFD) and scale model experiments [1].

The ultimate objective of the environmental control for a building is to ensure satisfactory thermal comfort and indoor air quality for the occupants and adequate heat distributions in winter and summer months.

The related literature work will be briefly summarized here. Khalili and Amindeldar [2] analyzed and investigated the low-energy solutions used in traditional architecture of Iran with an emphasis on dry and hot regions. Bahadori and Haghighat [3] studied natural ventilation due to wind effects through buildings employing domed roofs, having an opening at its crown, using flow network analysis. They determined that the domed roofs increase the air flow rate through the building. Laouadi and Atif [4] numerically studied laminar natural heat

transfer from multi-layer domes encountered in modern building designs. Correlations for the heat transfer as a function of the dome shape and the gap spacing between the layers were developed under steady-state conditions.

Tang et al. [5] studied heat transfer through a domed or vaulted roof using a 3D finite element model. This model allows a comparison of the thermal behavior of curved and flat roofs in terms of heat flux and daily heat flow through them into an air-conditioned building under different climatic conditions. Lin and Zmeureanu [6] studied a 3-D thermal and air flow (3D-TAF) model that estimates the energy needs of a dome-covered house where the model was verified with CFD simulations using the COMSOL software, experimental measurements. They indicated that the use of dome reduces the annual heating load of the house by 62.6%, compared with that of an isolated house located in Montreal at 45N latitude. In a follow up study, the authors investigated 3D thermal and airflow model that predicts the impact of such dome on the heating load of the protected house. The study involved a case study of a dome located in Montreal (Canada) [7].

Faghih and Bahadori [8] studied the thermal performance of domed roofs to determine the maximum air temperature of interior of buildings during the warm seasons. They showed that the thermal performance of domed roofs is better than the buildings with flat roof, particularly when the dome is covered with glazed tiles. Hussain and Oosthuizen [9] numerically studied the use of solar-assisted buoyancy-driven natural ventilation in a simple atrium building with particular emphasis on the thermal comfort conditions in the building. The authors used Reynolds Averaged Navier–Stokes (RANS) modeling approach with the SST k–ω turbulence model and the Discrete Transfer Radiation Model (DTRM). They noted that an atrium space integrated with a solar chimney would be a relatively better option to be used in an atrium building.

Bairi and García de María [10] numerically and experimentally studied natural convection in a hemispherical air-filled cavities with a circular base which is subjected to a constant heat flux for $10^4 \leq Ra \leq 5 \times 10^7$. The domical wall is maintained isothermal at a lower temperature which behaves as cold wall. Differences between the numerical and experimental results are reported to be relatively low staying always within the uncertainties of the experimental data. Correlations between average Nusselt and Rayleigh numbers are proposed to quantify the convective exchanges for engineering applications. Baïri et al. [11] studied numerically (using a 2D model) and experimentally the assemblies contained in hemispherical air-filled cavities whose disk is isothermal and inclined at an angle varying between 90 to 180 degrees for $10^4 \leq Ra \leq 5 \times 10^8$. Bairi [12] also examined the thermal and dynamical aspects of natural convection occurring in tilted hemispherical cavities whose disk is the active wall. The influence of the Rayleigh Number, the disk inclination angle and the thermal boundary condition on the disk is investigated numerically using a 2D model. Correlations that allow quantifying the heat transfer are proposed.

Bairi and Öztop [13] studied free convective heat transfer in hemispherical air-filled cavities. The numerical solution is obtained by finite volume method for Rayleigh numbers in the range $10^4 - 5 \times 10^8$. Numerical calculations are confirmed by measurements, leading to new Nusselt–Rayleigh type correlations. Zhang et al. [14] studied using a 3D numerical model for mixing and thermal stratification occurring in passive containment cooling systems.

Oztop et al. [15] studied thermal and flow fields due to natural convection of in curvilinear enclosures for different geometries using nanofluids. It is observed that curvilinear surface is the main effective parameter on heat and fluid flow in a nanofluid filled enclosure due to natural convection.

Large buildings with domes or curved roofs are generally encountered in unique buildings where novel ideas are also experimented. Thus, there exists no previous experience on the ventilation and heat distribution. As presented, current literature on this topic is very limited and most numerical models involve relatively small Ra numbers where the flow can be described as laminar. The laminar models are far from the actual structure ranges and cases of higher Ra numbers where turbulent flow is valid need to be studies. Thus, the objective of this study is to numerically investigate the flow of air and heat transfer in domical and/or curved buildings.

DESCRIPTION OF THE PROBLEM

Two- and three-dimensional geometry of the curved and domical structures considered in this study are presented in Figure 1. Two-dimensional enclosure is typical of observed in shopping malls, stations, theaters, factory building, etc where two-dimensional analysis is valid. The hot (T_h) and cold (T_c) faces are isothermal, and all the other walls are assumed to be adiabatic. The three-dimensional enclosures are observed in sport arenas and mostly in the middle eastern structures, including relatively small size mosques. The aspect ratio, H/L, is defined as the ratio of heated face height to the base face length. The models with $H/L=1$ and $H/L=2$ are considered for
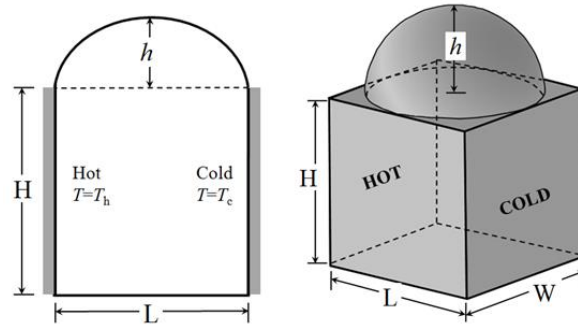
Figure 1. Two (a) and three (b) dimensional geometric models

both two- and three-dimensional ($L=W$) models. The curve or dome aspect ratio is defined as h/H which only $h/H =0.5$ is examined in the study. The enclosures are filled with air (Pr=0.71) and thermally driven on two vertically opposite faces.

GOVERNING EQUATIONS

In this numerical study, FLUENT® 6.3.26 [16] which nowadays is extensively used and repeatedly verified in academic and commercial research was used. The governing flow and energy equations, and the major features of the turbulence model will be briefly presented here to save space. The fluid flow is described by the Reynolds-Averaged Navier–Stokes (RANS) equations, including the averaged energy equation for the mean temperature field which drives the flow by the buoyancy force. Employing the Boussinesq approximation, the RANS equations for the continuity, momentum and energy conservation—using tensor notation—are reduced to the following:

$$\frac{\partial u_j}{\partial x_j} = 0, \tag{1}$$

$$\frac{Du_i}{Dt} = -\frac{1}{\rho}\frac{\partial P}{\partial x_i} - g_i\,\beta\,(T-T_r) + \frac{\partial}{\partial x_j}\left(\upsilon\frac{\partial u_j}{\partial x_j} - \overline{u_i u_j}\right), \tag{2}$$

$$\frac{DT}{Dt} = \frac{\partial}{\partial x_j}\left(\alpha\frac{\partial T}{\partial x_j} - \overline{T'u_j}\right), \tag{3}$$

where D/Dt is the material derivative, T is the temperature, T_r is a reference temperature, P is the pressure, g_i is the component of gravitational acceleration, β is the thermal expansion coefficient, ρ is the fluid density, α is the thermal diffusivity, υ is the kinematic viscosity and $\overline{u_i u_j}$ and $\overline{T'u_j}$ are the turbulent stress and heat flux which are supplied by the turbulence models. The Rayleigh number is defined with respect to the heated face height as $Ra_H=g\beta\Delta TH^3/\alpha v$. Boundary conditions are

on all faces, no-slip boundary condition ,u_j=0

on hot and cold faces, isothermal temperatures $T=T_h$ and $T=T_c$

on adiabatic faces, $\partial T/\partial n=0$

where n, h, and c refer to the normal direction to the face, hot and cold, respectively.

NUMERICAL ASPECTS

In this study, the RNG turbulence model available as a standard feature in FLUENT[R] was adapted due to its ability to capture the effects of swirl, high streamline curvature and transitional flows. The continuity, momentum and pertinent RNG $k-\varepsilon$ turbulence equations as well as the energy equation were solved using FLUENT. The numerical method that FLUENT employs is based on the finite volume method (FVM). The second-order accurate discretization to the transport terms, and similarly for the transient terms also second order implicit scheme was employed. The convergence criteria for all equations was 10^{-5}. To determine the effective time step size, $\Delta t \leq H^2/(4\alpha\sqrt{Ra\,Pr})$ expression suggested by FLUENT was used [16].

In order to obtain accurate and meaningful numerical solution, proper meshing the computational domain is crucial. The effects of meshing is more pronounced especially in fast moving flows due to steep temperature and velocity gradients occurring within the boundary layers. For the near-wall model, Enhanced Wall Treatment (EWT) was used which require meshing to be in the order of $y^+\approx1$. For this reason, to accurately resolve these steep gradients in the buoyancy-driven boundary layers and also satisfy y^+ criteria, different grid configurations involving fine meshes near the walls were used.

The heat transfer predictions from the enclosures are analyzed by computing the mean Nusselt number as area-weighted-average over the hot wall; that is,

$$\overline{Nu} = \frac{\bar{h}H}{k} = \frac{1}{A}\iint_A Nu\, dA, \tag{4}$$

where $\bar{h}$ is the mean convection heat transfer coefficient, H is the height of the heated face, k is the conductivity of air and A is the area of the hot face.

RESULTS AND DISCUSSION

The objective of this study is to study the thermal performance of curved and/or domed roofs in order to determine how they can be helpful in reducing the maximum air temperature of inside buildings during the warm seasons. Extensive studies on laminar natural convection in various enclosures have been carried out. Similarly very limited studies involve curved enclosures as indicated in the Introduction section. The studies involve relatively small Rayleigh numbers which are out of the range of building and structures which can be used for. The real building enclosures in mind, the working fluid is air. The geometries with *H/L=1* and *H/L=2* with curve aspect ratio *h/H*=0.5 are considered for $10^8 \leq Ra \leq 10^{10}$. The transient numerical simulations are performed since for high Rayleigh number cases do not converge steady state solutions even for turbulent flow models.

Flow and Heat Transfer in Two-Dimensional Cases

The variations of streamlines and isotherms of H/L=1 case are depicted for $Ra=10^8$, 10^9, and 10^{10} in Figure 2. The streamlines depict counter-clockwise rotation.

In Figure 2a, for $Ra=10^8$, the hot air plume is observed on the left side of the curved face on the top. As the Rayleigh number increases this plume proceeds to occupy the upper domain (Figure. 2c). The core of the circulation in this portion is relatively small in magnitude. Due to fast moving fluid, the streamlines in the vertical and horizontal faces are retract towards the wall faces.

The velocity boundary layers are thin, but with increasing Rayleigh number, the boundary layers on both cold and hot faces become thinner as expected. The streamlines below the heated and cooled faces take the rectangular form. The isotherms, in all three *Ra* cases, are parallel to the bottom face, as observed in the rectangular enclosures. The isotherms depict distortions on the vertical faces due to shear stresses produced by ascending and descending air. The thermal boundary layers are also observed to be very thin, and these boundary layers tend to become thinner with increasing Rayleigh numbers which imply increasing temperature gradients, consequently, increasing heat transfer rates. The hotter air is collected in the upper portion of the curved domain while the fluid circulates in the bottom square domain.

The variations of streamlines and isotherms of H/L=2 case are depicted for $Ra=10^8$, 10^9 and 10^{10} in Figure 3. This configuration is taller. The streamlines depict similar counter-clockwise rotation. In Figure 3a, for $Ra=10^8$, the hot air plume occupies the top curved domain. However, as the Rayleigh number increases the air plume moves towards the center of the upper domain (Figure 3b, 3c).

Due to high Rayleigh numbers, the air velocity is stronger in the vicinity of both lateral surfaces. As the streamlines concentrate on both vertical and horizontal faces, the velocity boundary layers become thinner with increasing Rayleigh number. Since the enclosure is thinner (H/L=2) in comparison to H/L=1 case, the effects of the shear stresses caused by ascending and descending air on cold and hot faces are more distinguishable. As expected, the thermal boundary layers on both lateral faces also become thinner. Away from the lateral faces, the streamlines and isotherms become flat and parallel to the bottom face in all three *Ra* cases. The hot air is similarly collected in the upper portion of the curved domain and the fluid circulating at the bottom rectangular domain remains strong.
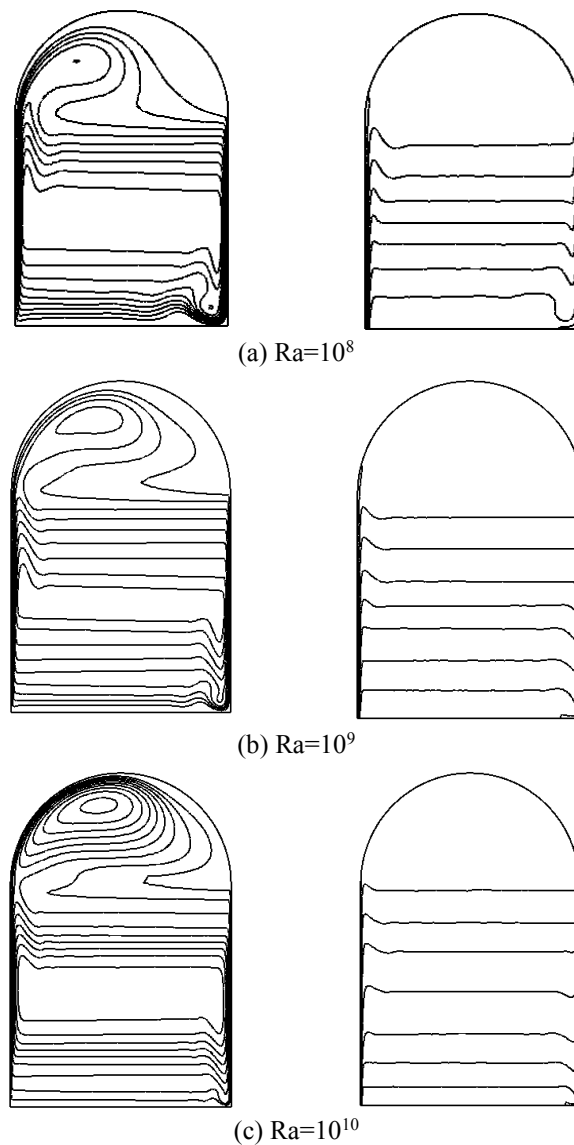
(a) Ra=10^8

(b) Ra=10^9

(c) Ra=10^{10}

Figure 2. The variation of stream lines (left) and isotherms (right) with Rayleigh number for H/L=1 case

Flow and heat transfer in three-dimensional cases

The variations of flow (thru pathlines colored by temperature) and isotherms of H/L=1 case are depicted for $Ra=10^8$, and 10^{10} in Figure 4. Due to the three-dimensionality of the flow, the flow sufficiently away from the walls, especially at the bottom cubic zone, tends to behave as in the 2-D cases.

However, at the upper hemispherical domain in Figure 4a, for $Ra=10^8$, the flow is confined to the left portion of the hemisphere and the pathlines depict three-dimensional flow while the cold face side of the upper hemisphere remain relatively intact. Pathlines are concentrated near the cold and hot walls while the core of the cubic zone is relatively motionless which yields horizontally layered temperature distribution from bottom face to the top. In Figure 4b, for $Ra=10^{10}$, no pathlines are observed at the interior zone. The air flow completely retracts to the enclosure faces while the top surface of the dome does not interact with the flow. The flow is mostly confined to the bottom portion of the dome as circular motions. Since the front and back faces which are adiabatic does help the horizontally layered temperature distribution; however, the fluid in the vicinity of these walls lose momentum; thus, the flow field is distorted.

The variations of flow (thru pathlines colored by temperature) and isotherms of H/L=2 case are depicted for $Ra=10^8$ and 10^{10} in Figure 5. Similar trend is also observed here where hot air plume is created on the hotter side of the domewhich occupied a vast region (Figure 5a), but with increasing Rayleigh number the flow rotation retracts to left surface of the dome.
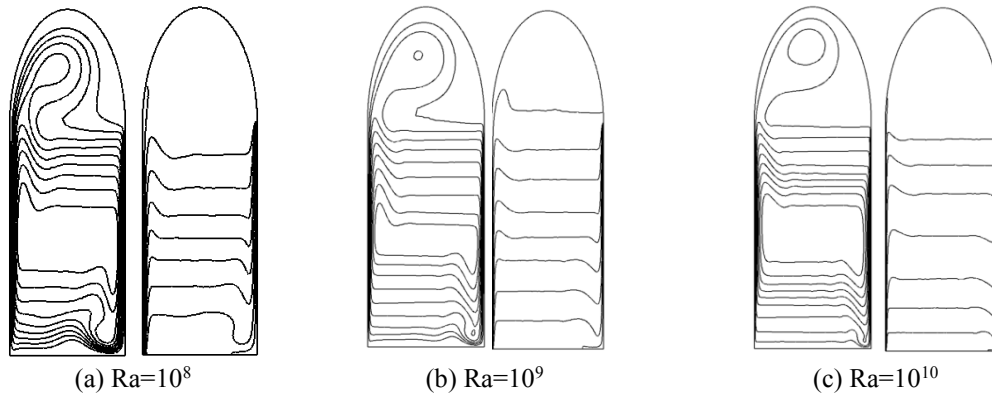
(a) Ra=10^8 (b) Ra=10^9 (c) Ra=10^{10}

Figure 3. The variation of stream lines (left) and isotherms (right) with Rayleigh number for H/L=2 case
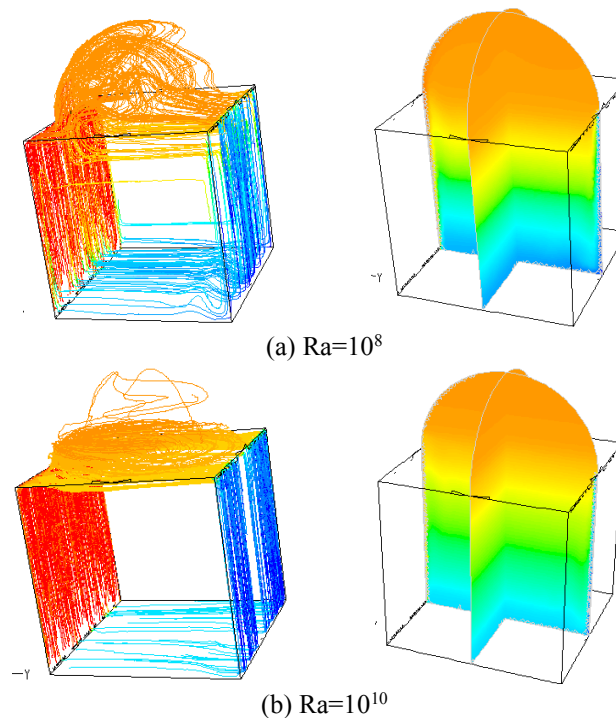

(a) Ra=10^8

(b) Ra=10^{10}

Figure 4. For H/L=1, path lines colored by static temperature (left) and isotherms (right) for *x*=0.5 and *y*=0.5 planes

Pathlines are concentrated near the cold and hot walls; however, as the pathlines similar to streamlines in 2D are observed for *Ra*=10^8, these pathlines disappear in *Ra*=10^{10}. For increasing *Ra* numbers, the air flow completely retracts to the enclosure faces. Since there are heat losses from the front and back faces, temperature distributions likewise becomes horizontally layered.

The mean Nusselt numbers computed over the hot surface using two and three-dimensional models are tabulated in Table 1 along with Catton and Bairi's correlations for rectangular enclosures (flat top face). Catton [17] recommends *Nu*=0.18 *(Pr Ra/(Pr+0.2))*$^{0.29}$. In his two-dimensional numerical analysis, Bairi [18] develops the following mean Nusselt number correlation: *Nu*=0.14 *Ra*$^{0.30}$. Our 2-D computational mean Nusselt results yield identical solutions for *H/L*=1, and 2 which means that the heat transfer rate is not significantly altered with *H/L* ratio. On the other hand, our results are relatively smaller than those of both Cotton and Bairi. However, the 3-D model results yield higher mean Nusselt solutions in comparison to 2-D models which signifies the 3-D flow effects. This indicate that the thermal boundary layer is influenced due to the presence of the curved top surfaces (especially at the upper zone of the heated face) where hot air is accumulated. Thus the heat transfer to the.
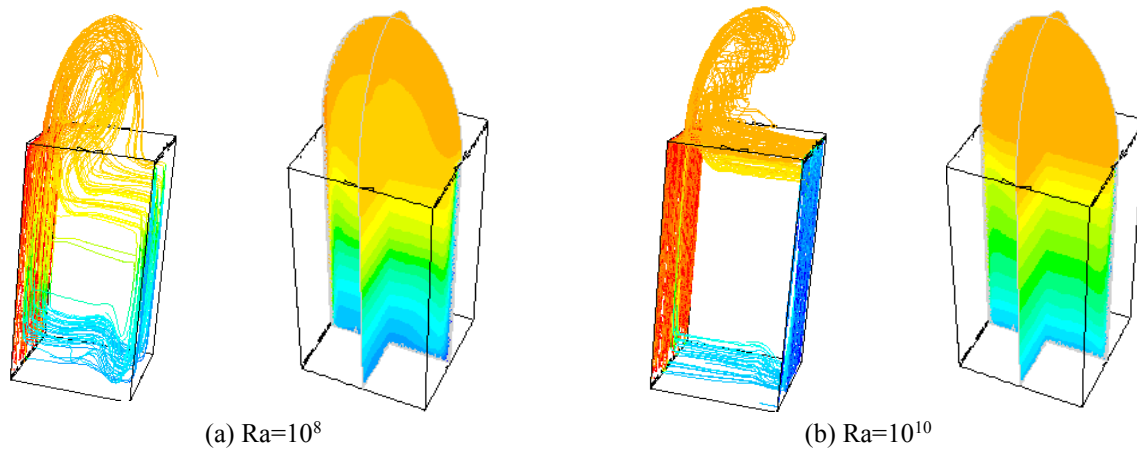
(a) Ra=10^8 (b) Ra=10^{10}

Figure 5. For H/L=2, path lines colored by static temperature (left) and isotherms (right) for *x*=0.5 and *y*=0.5 planes

enclosure is reduced in comparison to flat top surface. This means that the thermal performance of the investigated curved and domed roofs is better than the building with flat roof since the warm air is collected in the upper zones leading cooler circulations in the zones beneath it

Table 1. The mean Nusselt numbers computed using 2D and 3D models.

Ra	Catton [17]	Bairi [18]	H/L=1		H/L=2	
			2D	3D	2D	3D
10^8	35	35,1	30,2	30,3	30,7	32,03
10^9	68,2	70,1	54,3	73,94	55,2	66,59
10^{10}	133,1	140	102,3	101,6	103,4	134,9

Finally, we must add that the performance of the top surface (roof) depends mainly on its form, construction and materials. Generally when the roof surface is protected from the direct warming effect of solar rays, heat gain is minimal.

CONCLUSION

In this study, transient buoyancy driven free convection heat transfer in curved or domical structures is investigated numerically using two- and three-dimensional turbulent models in the interval $10^8 \leq Ra \leq 10^{10}$. The aspect ratios of *H/L*=1, and 2 are considered as the heating and cooling is provided from a lateral faces. The flow and temperature fields at the top zone of the enclosures are altered. The hot air is collected at the curved/or domical zones where the circulation is weak. In the rectangular zones the flow and temperature fields are similar to those of rectangular (flat top) domains. The mean Nusselt number evaluated from 2-D simulations indicate that the mean Nusselt number with *H/L* ratio does not significantly change, but a significant increase is observed with increasing Ra numbers. 3-D simulations yield higher mean Nusselt numbers but they are smaller than those of flat top enclosures.

NOMENCLATURE

H   The heated face height
L   The base face length
W   The base face depth
Ra   Rayleigh number
Nu   Nusselt number
ρ   Density of the air
k   Turbulent kinetic energy
ε   Turbulent dissipation rate

h	The height of the dome
T_r	Reference temperature
β	Thermal expansion coefficient
P	Pressure
g_i	The component of gravitational acceleration
T	Temperature
$\overline{u_i u_j}$	The turbulent stress
$\overline{T' u_j}$	The heat flux
α	The thermal diffusivity
ν	The kinematic viscosity
u	Velocity
A	The area of the hot face

REFERENCES

[1] P. Heiselberg, S. Murakami, and C. Roulet, "Ventilation of large spaces in buildings: Analysis and Prediction Techniques", IEA, Energy Conservation in Buildings and community Systems, Annex 26: Energy Efficient Ventilation of Large Enclosures. Kolding Trykcenter A/S, Denmark, 1998.

[2] M. Khalili, S. Amindeldar, "Traditional solutions in low energy buildings of hot-arid regions of Iran", Sustainable Cities and Society, vol. 13, pp. 171-181, 2014.

[3] M.N. Bahadori and F. Haghighat, "Passive cooling in hot, arid regions in developing countries by employing domed roofs and reducing the temperature of internal surfaces", Building and Environment, vol. 20 (2), pp. 103-113, 1985.

[4] A. Laouadi and M. R. Atif, "Natural convection heat transfer within multi-layer domes", International Journal of Heat and Mass Transfer, vol. 44(10), pp. 1973-1981, 2001.

[5] R. Tang, I.A. Meir, and Y. Etzion, "Thermal behavior of buildings with curved roofs as compared with flat roofs", Solar Energy, vol. 74(4), pp. 273-286, 2003.

[6] Y. Lin and R. Zmeureanu, "Three-dimensional thermal and airflow (3D-TAF) model of a dome-covered house in Canada", Renewable Energy, vol. 33(1), pp. 22-34, 2008.

[7] Y. Lin and R. Zmeureanu, "Computer model of the airflow and thermal phenomena inside a large dome", Energy and Buildings, vol. 40(7), pp. 1287-1296, 2008.

[8] A.K. Faghih and M. N. Bahadori, "Thermal performance evaluation of domed roofs", Energy and Buildings, vol. 43(6), pp. 1254-1263, 2011.

[9] S. Hussain and P. H. Oosthuizen, "Numerical investigations of buoyancy-driven natural ventilation in a simple atrium building and its effect on the thermal comfort conditions", Applied Thermal Engineering, vol. 40, pp. 358-372, 2012.

[10] A. Baïri and J. M. García de María, "Numerical and experimental study of steady state free convection generated by constant heat flux in tilted hemispherical cavities", International Journal of Heat and Mass Transfer, vol.66, pp. 355-365, 2013.

[11] A. Baïri, E. Monier-Vinard, N. Laraqi, I. Baïri, M.N. Nguyen, and C.T. Dia, "Natural convection in inclined hemispherical cavities with isothermal disk and dome faced downwards. Experimental and numerical study", Applied Thermal Engineering, vol. 73(1), pp. 1340-1347, 2014.

[12] A. Baïri, "A synthesis of correlations on quantification of free convective heat transfer in inclined air-filled hemispherical enclosures", International Communications in Heat and Mass Transfer, vol. 59, pp. 174-177, 2014.

[13] A. Baïri and H.F. Öztop, "Free convection in inclined hemispherical cavities with dome faced downwards. Nu–Ra relationships for disk submitted to constant heat flux", International Journal of Heat and Mass Transfer, vol. 78, pp. 481-487, 2014.

[14] H. Zhang, F. Niu, Y. Yu, S. Zhang, H. Wang, and Z. Gang, "Modeling and experimental studies on mixing and stratification during natural convection in containments", Annals of Nuclear Energy, vol. 85, pp. 317-325, 2015.

[15] H.F. Oztop, F. Selimefendigil, E. Abu-Nada, and K. Al-Salem, "Recent developments of computational methods on natural convection in curvilinear shaped enclosures", *Journal of Thermal Engineering*, vol. 2(2), pp. 693-698, 2016.

[16] Fluent 6.3 Users' Guide, Fluent Inc., Lebanon, NH, 2006.

[17] I.Catton, "Natural Convection in Enclosures", *Proc. 6th Int. Heat Transfer Conf.*, Toronto, Canada, pp. 13–31, Vol. 6, Press,1978.

[18] A. Baïri, "Nusselt–Rayleigh correlations for design of industrial elements: Experimental and numerical investigation of natural convection in tilted square air filled enclosures", *Energy Conversion and Management*, vol.49 (4), pp. 771-782, 2008.